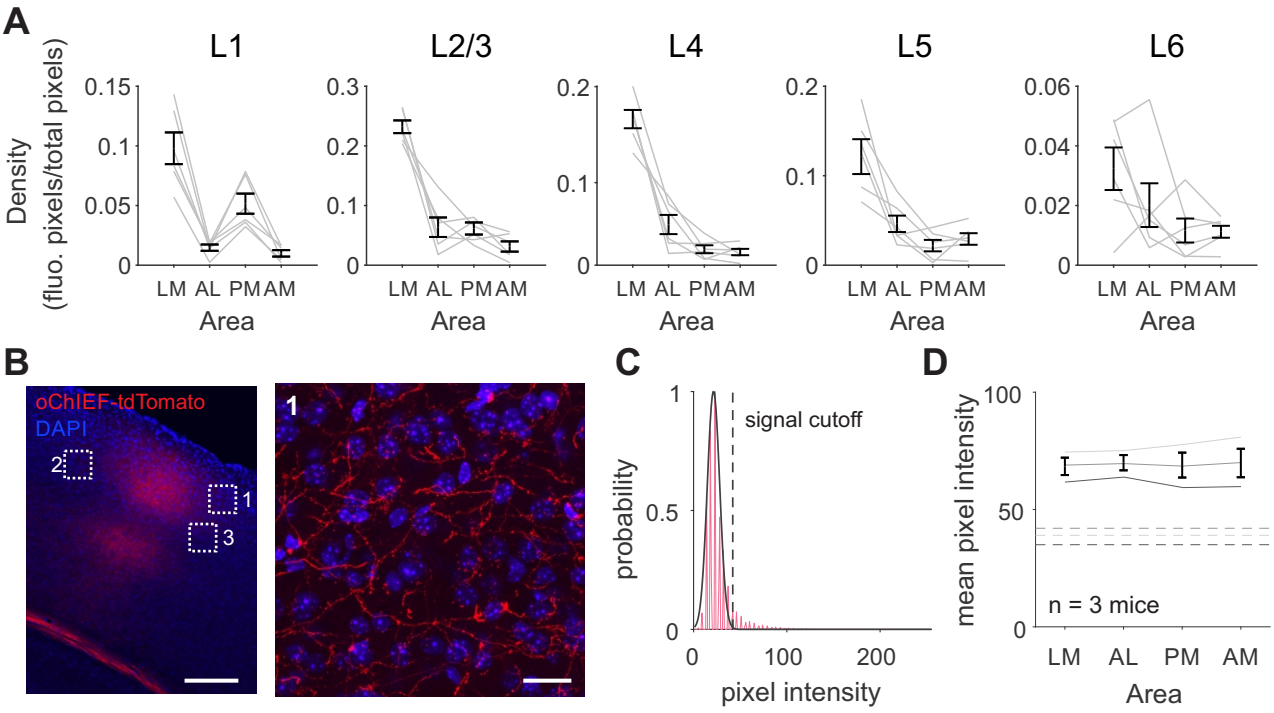

Figure S1. Non-normalized fluorescence densities and single axon fluorescence intensities, related to Figure 2. A. Non-normalized axon fluorescence density by area for L1-L6 (left to right). Gray lines are individual animals, black lines are mean across animals for each area and layer. Error bars are SEM across animals. **B.** Left: 10x example image of AL and 3 regions selected for higher magnification analysis. Scale bar is 200 µm. Right: 63x example image in area labeled region 1. Scale bar is 25 µm. **C.** Pixel intensity distribution for example animal in **B (**pooled across areas; red). Signal cutoff (dashed line) was set at 1 FWHM above the peak of a Gaussian fit to the distribution (black curve). **D.** Mean pixel intensities within each area across animals (gray lines). Dashed lines indicate signal cutoff for each animal, colored by animal. Black lines are mean SEM across animals.

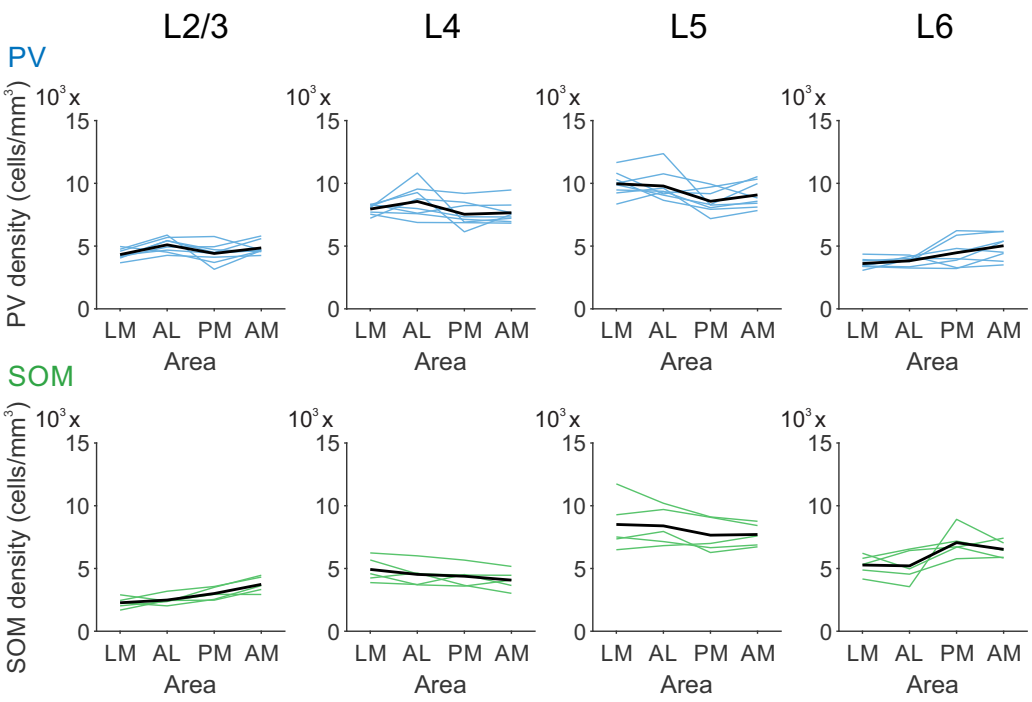

Figure S2. Raw PV and SOM cell densities by area, related to Figure 3. Top: Raw PV cell density by area for L2/3-L6 (left to right). Colored lines indicate individual animals, black line indicates mean across animals. Bottom: Same as top for SOM cells.

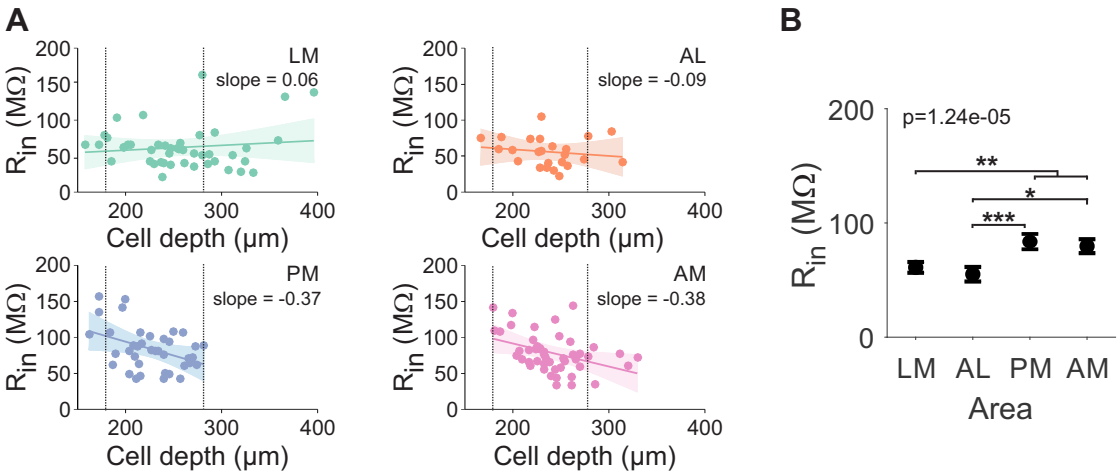

Figure S3. Pyramidal cell R_{in} by cell depth, related to Figure 4. A. R_{in} by recorded cell depth from pia for LM, AL, PM, and AM. Colored circles are individual neurons. Vertical dashed line indicates bounds for matching cells by depth. Shading indicates 95% condfidence interval of linear fit. **B.** Average R_{in} by area using only depth-matched cells (LM n = 28, AL n = 28, PM n = 47, AM n = 57). Error is SEM across cells. *,**, and *** denote $p < 0.05, 0.01$, and 0.001.

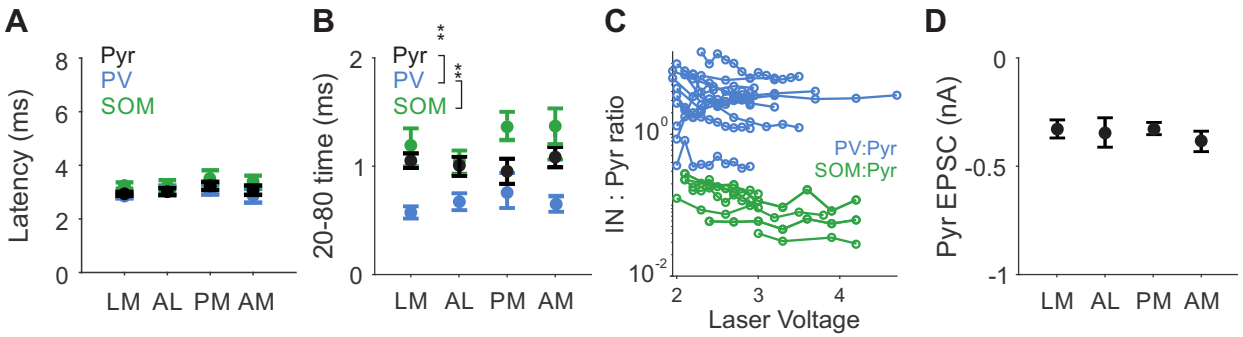

Figure S4. Temporal dynamics and stability of optogenetically-evoked EPSCs, related to Figures 5-6. A. Latency (time to 20% peak) of EPSCs by cell type and area. No significant effect of area or cell type. Error is SEM across cells. **B.** 20-80% rise time of EPSCs by cell type. No significant effect of area, significant effect of cell type (PV vs Pyr, $p<0.001$; PV vs SOM, $p<0.001$; two-way ANOVA with post-hoc Tukey test). **C.** IN:Pyr ratios for PV:Pyr (blue) and SOM:Pyr (green) pairs as a function of laser intensity. Lines connect IN:Pyr ratios from the same pairs across laser intensities. **D.** Raw pyramidal cell EPSC amplitude by area.

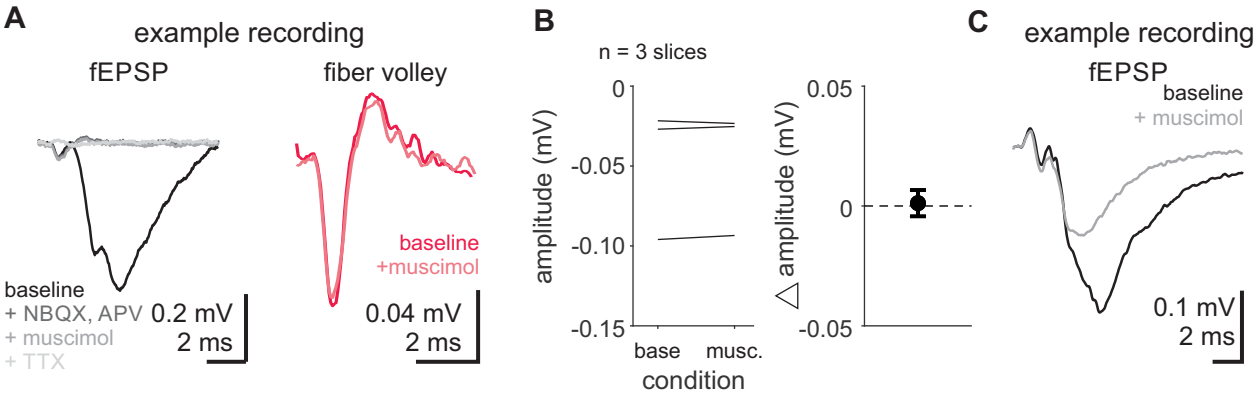

Figure S5. Muscimol blocks late-onset activation without affecting fiber volley, related to Figures 5-6. A. Example field recording of the fiber volley is not affected by muscimol. Left: baseline (black) field excitatory postsynaptic potential (fEPSP) in the presence of $GABA_B$ receptor antagonist CGP54626. Application of glutamate receptor antagonists (NBQX and APV; dark gray) blocked the synaptic conductance leaving the fiber volley (medium grays) which is blocked by tetrodoxin (TTX; light gray). Right: fiber volley before (red) and after (pink) muscimol. **B.** Left: Raw amplitude of fiber volley before and after muscimol application. Right: Summarized change in amplitudes. Error is SEM across experiments. There is no effect of muscimol on the fiber volley (paired t-test; $p = 0.953$) **C.** Example fEPSP in the presence of $GABA_B$ receptor antagonist (black) and after muscimol (gray). Note that muscimol abolishes the late component of the fEPSP.

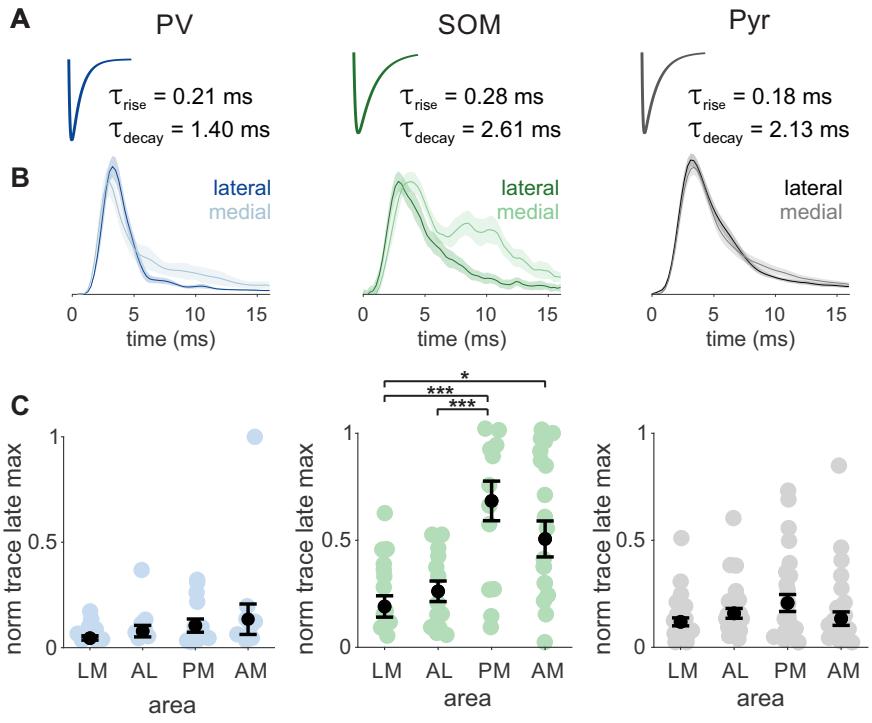

Figure S6. Deconvolution of PV, SOM, and Pyr EPSCs with EPSC templates from spontaneous activity, related to Figure 6. A. Templates used for deconvolution were fit from spontaneous EPSCs recorded in each cell type. Templates were not significantly different between areas so EPSCs were grouped to generate a single template for each cell type. **B.** Average deconvolved activity grouped by medial (dark) and lateral (light) areas, normalized to the maximum response. Shaded error is SEM across cells. **C.** Maximum normalized response in the late time window post-monosynaptic inputs (7.5-15 ms). Colored circles - individual cells; black circles - mean. Error is SEM across cells.*,**, and *** denote $p < 0.05, 0.01$, and 0.001.

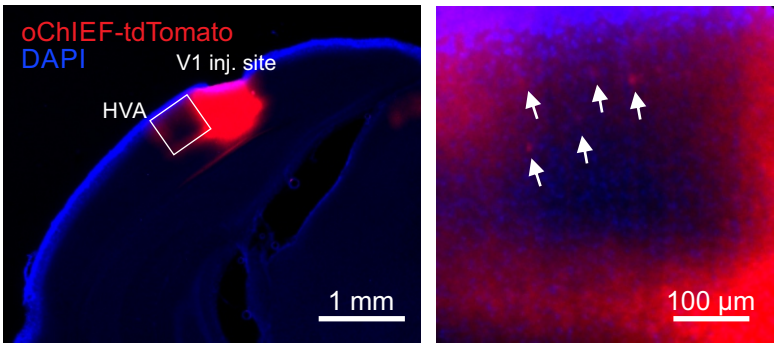

Figure S7. Example slice exhibiting transsynaptic labeling, related to STAR Methods and Figures 2-7. Example slice with cell bodies labelled (arrows) outside of the injection site in an oChIEF-injected animal. Labeling may be either via viral uptake by HVA axons in V1, or expulsion of viral particles from V1 axons. Data from experimental days with this type of labeling was excluded.

	Pyr (n = 153)	**PV** (n = 80)	**SOM** (n = 83)
R_{in} (MΩ)	87.79 ± 26.31	104.66 ± 27.96	151.32 ± 43.75
AP width (ms)	0.83 ± 0.21	0.31 ± 0.07	0.50 ± 0.14
AP adapt	0.18 ± 0.05	0.87 ± 0.12	0.46 ± 0.15
Membrane tau (ms)	8.62 ± 2.85	6.59 ± 1.72	20.22 ± 7.26
Sag (mV)	2.12 ± 1.02	0.79 ± 0.52	3.12 ± 1.72

Table S1. Cell-intrinsic properties of Pyr, PV, and SOM cells across all HVAs, related to Figure 4. All data are mean ± SD.

	Pyr→ PV	Pyr →SOM	PV →Pyr	SOM →Pyr
Connected/Total	47/117 = 0.40	42/86 = 0.49	82/117 = 0.70	58/86 = 0.67
P1 amplitude (pA)	-21.06 ± 2.65	-16.49 ± 2.42	27.81 ± 2.34	16.71 ± 1.92
P2/P1	0.96 ± 0.07	1.02 ± 0.08	0.81 ± 0.04	0.88 ± 0.03
P10/P1	0.87 ± 0.05	1.83 ± 0.15	0.66 ± 0.04	0.85 ± 0.04

Table S2. Connectivity parameters grouped across areas for PV/SOM and Pyr cell types, related to Figure 7. Table of amplitude and paired-pulse ratio of Pyr and IN connections across all HVAs. Data are mean ± SEM.